

# Supersymmetric model contributions to $B_d^0-\bar{B}_d^0$ mixing and $B \rightarrow \pi\pi, \rho\gamma$ decays

A. Arhrib, C.-K. Chua, W.-S. Hou

Department of Physics, National Taiwan University, Taipei, Taiwan 10764, R.O.C.

Received: 12 April 2001 / Revised version: 7 July 2001 /

Published online: 24 August 2001 – © Springer-Verlag / Società Italiana di Fisica 2001

**Abstract.** Recent results from the Belle and BaBar Collaborations hint at a small  $\sin 2\phi_1$ , while the measured  $B \rightarrow \pi\pi$  rate also seems to be on the low side. Supersymmetric (SUSY) models with down squark mixings can account for the deficits in both cases. By studying the origin of SUSY contributions that could impact on  $B_d^0-\bar{B}_d^0$  mixing and  $B \rightarrow \pi\pi$  decay, we find that the former would most likely arise from left–left or right–right squark mixings, while the latter would come from left–right squark mixings. These two processes in general are not much correlated in the minimum supersymmetric standard model. If the smallness of  $B \rightarrow \pi\pi$  is due to SUSY models, one would likely have a large  $B \rightarrow \rho\gamma$  from chiral enhancement, and the rate could be within the present experimental reach. Even if  $B \rightarrow \rho\gamma$  is not greatly enhanced, it could have large mixing dependent  $CP$  violation.

## 1 Introduction

The  $CP$  asymmetries in  $B^0 \rightarrow J/\psi K_S, J/\psi K_L$  decays have been studied by several experimental groups [1–5]. It is well known that one of the phase angles of the standard model (SM) unitarity triangle,  $\sin 2\phi_1$ , can be measured via the asymmetry,

$$a_{J/\psi K_S} = \frac{\Gamma(B^0(t) \rightarrow J/\psi K_S^0) - \Gamma(\bar{B}^0(t) \rightarrow J/\psi K_S^0)}{\Gamma(B^0(t) \rightarrow J/\psi K_S^0) + \Gamma(\bar{B}^0(t) \rightarrow J/\psi K_S^0)} = -\sin 2\phi_1 \sin \Delta m_{B_d} t. \quad (1)$$

The CDF Collaboration finds  $\sin 2\phi_1 = 0.79_{-0.44}^{+0.41}$  [1] with Tevatron Run-I data, while the OPAL and ALEPH Collaborations give  $\sin 2\phi_1 = 3.2_{-2.0}^{+1.8} \pm 0.5$  [2],  $0.84_{-1.04}^{+0.82} \pm 0.16$  [3], respectively. Recently, however, the BaBar and Belle Collaborations announced their results on the measurement of this asymmetry. The Belle Collaboration reports  $\sin 2\phi_1 = 0.58_{-0.34-0.10}^{+0.32+0.09}$  [4], while the BaBar Collaboration gives the even smaller  $\sin 2\phi_1 = 0.34 \pm 0.20 \pm 0.05$  [5]. When combined with previous CDF and LEP results, the average value is  $\sin 2\phi_1 = 0.48 \pm 0.16$ . While this is consistent with the Cabibbo–Kobayashi–Maskawa (CKM) fit value of  $\sin 2\phi_1 = 0.698 \pm 0.066$  [6] or  $0.47 \leq \sin 2\phi_1 \leq 0.93$  (95% C.L.) [7], the central value is rather small. This could be hinting at the presence of new physics effects, especially if the value persists. In this case, we may need a large new physics contribution [8] in  $B^0-\bar{B}^0$  mixing, comparable to the SM amplitude, to account for the smallness of  $a_{J/\psi K_S}$ . This is because it is very hard for new physics to affect the Cabibbo favored  $b \rightarrow c\bar{c}s$  decay amplitude.

The first result on the charmless decay mode  $B^0 \rightarrow \pi^+\pi^-$  was given by the CLEO Collaboration, giving

$\text{Br}(B^0 \rightarrow \pi^+\pi^-) = (4.3_{-1.4}^{+1.6} \pm 0.5) \times 10^{-6}$  [9]. The BaBar and Belle Collaborations also recently reported their results,  $\text{Br}(B^0 \rightarrow \pi^+\pi^-) = (4.1 \pm 1.0 \pm 0.7) \times 10^{-6}$  [10],  $(5.9_{-2.1}^{+2.4} \pm 0.5) \times 10^{-6}$  [11], respectively. Note that the BaBar and Belle measurements are all lower than their reported results at the summer 2000 conferences [12,13]. The combined result with averaged  $\text{Br}(B^0 \rightarrow \pi^+\pi^-) = 4.4 \pm 0.9$  seems to be on the low side when compared to the SM prediction using the factorization approach,  $\text{Br}(B^0 \rightarrow \pi^+\pi^-) \sim 10 \times 10^{-6}$  [14], for  $\phi_3 \sim 60^\circ$ , and remains true when compared to the QCD factorization result [15] of  $\text{Br}(B^0 \rightarrow \pi^+\pi^-) \sim 8 \times 10^{-6}$ . In a recent work on QCD factorization,  $\text{Br}(\pi^+\pi^-)$  can turn out to be close to the experimental value; however, the smallness of the rate would subject the SM to considerable stress [16]. A 20%–40% or more reduction in the branching ratio is welcome. In SM, the tree amplitude dominates over the penguin amplitude, which is about 30% of the former. Thus we may need a large contribution from new physics if it is responsible for the smallness of the rate.

We have two cases where we are in a situation that new physics contributions should be large, if it is responsible for the smallness of measurements. As one of the leading candidates for new physics, supersymmetry (SUSY) helps resolve many of the potential problems that emerge when one goes beyond the SM, for example the gauge hierarchy problem, unification of  $SU(3) \times SU(2) \times U(1)$  gauge couplings, and so on [17]. In the context of SUSY, we then ask the following questions: Is it possible for SUSY models to account for the smallness in both processes? If so, are they correlated, since both of them are  $b \rightarrow d$  flavor changing processes? Since new physics contributions would be large, can we find other related effects?

To analyse SUSY contributions, we follow the approach of [18]. As will be discussed later, gluino exchange diagrams induced by  $\tilde{d}-\tilde{b}$  mixings give dominant contributions in both of the above mentioned processes. We do not aim at constructing any explicit models; hence we have not considered other flavor changing processes such as  $K^0-\bar{K}^0$  mixing,  $D^0-\bar{D}^0$  mixing,  $\text{Br}(B \rightarrow X_s\gamma)$  and the neutron electric dipole moment, etc., since these are controlled by other parameters. Our strategy has been simply to study the implications on  $\tilde{d}-\tilde{b}$  squark mixings from new data on  $B_d$  mixing and  $B \rightarrow \pi\pi$  decay, and make inferences on other modes, such as  $B \rightarrow \rho\gamma$  which is quite correlated with effects in  $B \rightarrow \pi\pi$ . We have assumed that models can be constructed such that SUSY can impact on the modes considered here, but do not run into trouble with other stringent low energy constraints (see e.g. [8] for  $B_d$  mixing case).

We organize this paper in the following way: We discuss SUSY contribution to  $B^0-\bar{B}^0$  mixing,  $B \rightarrow \pi\pi$  and radiative  $B$  decays in the next two sections. We then give some discussion, followed by a conclusion in the last section.

## 2 $B^0-\bar{B}^0$ mixing in SUSY models

The effective Hamiltonian for  $B_d^0-\bar{B}_d^0$  mixing from SUSY contributions is given by

$$H_{\text{eff}} = -\sum_i C_i \mathcal{O}_i, \quad (2)$$

where

$$\begin{aligned} \mathcal{O}_1 &= \bar{d}_L^\alpha \gamma_\mu b_L^\alpha \bar{d}_L^\beta \gamma^\mu b_L^\beta, \\ \mathcal{O}_2 &= \bar{d}_L^\alpha b_R^\alpha \bar{d}_L^\beta b_R^\beta, \quad \mathcal{O}_3 = \bar{d}_L^\alpha b_R^\beta \bar{d}_L^\beta b_R^\alpha, \\ \mathcal{O}_4 &= \bar{d}_L^\alpha b_R^\alpha \bar{d}_R^\beta b_L^\beta, \quad \mathcal{O}_5 = \bar{d}_L^\alpha b_R^\beta \bar{d}_R^\beta b_L^\alpha, \end{aligned} \quad (3)$$

together with three other operators  $\tilde{\mathcal{O}}_{1,2,3}$  (and associated coefficients  $\tilde{C}_i$ ) that are chiral conjugates (L  $\leftrightarrow$  R) of  $\mathcal{O}_{1,2,3}$ . There are contributions from gluino, neutralino, charged Higgs and chargino exchange diagrams [19]. We note that, due to the Majorana property of the gluino, gluino exchange diagrams can be divided into the usual box diagram and the so-called crossed diagram. By using the double line notation of 't Hooft [20], it is easy to see that the former has a color factor  $N_c$ , while the latter does not. In general, therefore, the leading SUSY contribution comes from gluino box diagrams, where we have  $\alpha_s^2$  and  $N_c$  enhancement, although it is possible that in some parameter space, such as small  $\tan\beta$  and when superparticles are light, charged Higgs and chargino contributions may become important [21].

It is customary to take squarks as almost degenerate at scale  $\tilde{m}$ . In the following, we give contributions from gluino exchange diagrams and make use of the mass insertion approximation [18,22]. In the quark mass basis, one defines [22],

$$\delta_{qAB}^{ij} \equiv (\tilde{m}_q^2)^{ij} / \tilde{m}^2, \quad (4)$$

which is roughly the squark mixing angle,  $\tilde{m}_q^2$  are squark mass matrices,  $A, B = \text{L, R}$ , and  $i, j$  are generation indices. For notational simplicity, we shall suppress in what follows the index pair  $ij$  (13 for a  $\tilde{d}-\tilde{b}$  mixing angle) as well as the subscript  $d$ .

The gluino exchange contributions to the Wilson coefficients are [18],

$$\begin{aligned} C_1 &= \frac{\alpha_s^2}{\tilde{m}^2} \left[ \frac{1}{4} \left( 1 - \frac{1}{N_c} \right)^2 x_{\tilde{g}\tilde{q}} f_6(x_{\tilde{g}\tilde{q}}) \right. \\ &\quad \left. + \frac{1}{8} \left( N_c - \frac{2}{N_c} + \frac{1}{N_c^2} \right) \tilde{f}_6(x_{\tilde{g}\tilde{q}}) \right] \delta_{\text{LL}}^2, \\ C_2 &= \frac{\alpha_s^2}{\tilde{m}^2} \frac{1}{2} \left( N_c - 1 - \frac{1}{N_c^2} \right) x_{\tilde{g}\tilde{q}} f_6(x_{\tilde{g}\tilde{q}}) \delta_{\text{LR}}^2, \\ C_3 &= \frac{\alpha_s^2}{\tilde{m}^2} \frac{1}{2} \left( -1 + \frac{2}{N_c} \right) x_{\tilde{g}\tilde{q}} f_6(x_{\tilde{g}\tilde{q}}) \delta_{\text{LR}}^2, \\ C_4 &= \frac{\alpha_s^2}{\tilde{m}^2} \left\{ \left( -\frac{1}{2} - \frac{1}{N_c^2} \right) \tilde{f}_6(x_{\tilde{g}\tilde{q}}) \delta_{\text{LR}} \delta_{\text{RL}} \right. \\ &\quad \left. + \left[ \left( N_c - \frac{2}{N_c} \right) x_{\tilde{g}\tilde{q}} f_6(x_{\tilde{g}\tilde{q}}) - \frac{\tilde{f}_6(x_{\tilde{g}\tilde{q}})}{N_c} \right] \delta_{\text{LL}} \delta_{\text{RR}} \right\}, \\ C_5 &= \frac{\alpha_s^2}{\tilde{m}^2} \left\{ \left( \frac{1}{2N_c} - \frac{N_c}{2} \right) \tilde{f}_6(x_{\tilde{g}\tilde{q}}) \delta_{\text{LR}} \delta_{\text{RL}} \right. \\ &\quad \left. + \left[ \frac{x_{\tilde{g}\tilde{q}} f_6(x_{\tilde{g}\tilde{q}})}{N_c^2} + \left( \frac{1}{2} + \frac{1}{2N_c^2} \right) \tilde{f}_6(x_{\tilde{g}\tilde{q}}) \right] \delta_{\text{LL}} \delta_{\text{RR}} \right\}, \end{aligned} \quad (5)$$

where  $x_{\tilde{g}\tilde{q}} \equiv m_{\tilde{g}}^2 / \tilde{m}^2$ , and  $\tilde{C}_{1,2,3}$  are given by changing L  $\leftrightarrow$  R in  $C_{1,2,3}$ , respectively. As noted before, the terms containing  $N_c$  are from the box diagrams, while those containing 1 are from crossed diagrams and  $1/N_c, 1/N_c^2$  are from subleading terms of box and crossed diagrams. The loop functions are given by

$$\begin{aligned} [-\tilde{f}_6(x_{\tilde{g}\tilde{q}}), x_{\tilde{g}\tilde{q}} f_6(x_{\tilde{g}\tilde{q}})] &= \tilde{m}^6 \frac{\partial^2}{\partial \tilde{m}'^2 \partial \tilde{m}^2} \int_0^\infty dk^2 \\ &\times \left\{ \frac{k^2}{(k^2 + m_{\tilde{g}}^2)^2} \frac{[k^2, m_{\tilde{g}}^2]}{(k^2 + \tilde{m}^2)(k^2 + \tilde{m}'^2)} \right\} \Bigg|_{\tilde{m}' \rightarrow \tilde{m}}, \end{aligned} \quad (6)$$

which agrees with [18]. Note that  $f_6(x_{\tilde{g}\tilde{q}})$  is always positive, while  $\tilde{f}_6(x_{\tilde{g}\tilde{q}})$  is always negative. It is useful to give the asymptotic forms of these functions:

$$\begin{aligned} [-\tilde{f}_6(x_{\tilde{g}\tilde{q}}), x_{\tilde{g}\tilde{q}} f_6(x_{\tilde{g}\tilde{q}})] &= \begin{cases} [1/(3x_{\tilde{g}\tilde{q}}^2), 1/x_{\tilde{g}\tilde{q}}], & \text{for } \tilde{m} \ll m_{\tilde{g}} \ (x_{\tilde{g}\tilde{q}} \gg 1), \\ [1/30, 1/20], & \text{for } m_{\tilde{g}} = \tilde{m} \ (x_{\tilde{g}\tilde{q}} = 1), \\ [1/3, -x_{\tilde{g}\tilde{q}} \ln x_{\tilde{g}\tilde{q}}], & \text{for } m_{\tilde{g}} \ll \tilde{m} \ (x_{\tilde{g}\tilde{q}} \ll 1). \end{cases} \end{aligned} \quad (7)$$

By using these asymptotic forms, it is easy to show that  $|\tilde{f}_6(x_{\tilde{g}\tilde{q}})| < |x_{\tilde{g}\tilde{q}} f_6(x_{\tilde{g}\tilde{q}})|$  for  $\tilde{m} \ll m_{\tilde{g}}$  and vice versa. Therefore, one must have a zero in  $C_1$  ( $\tilde{C}_1$ ) for some value of  $x_{\tilde{g}\tilde{q}}$  and hence a sign change when passing through it. One can also show that the cancellation is between the above mentioned two class of diagrams.

After obtaining these Wilson coefficients at the SUSY scale  $M_{\text{SUSY}}$ , we apply renormalization group running to

**Table 1.** The input parameters used in this section

Parameter	Value	Parameter	Value
$\bar{\rho}$	0.169	$\bar{\eta}$	0.362
$f_{B_d}\sqrt{\hat{B}_{B_d}}$	$230 \pm 40$ MeV	$m_B$	5.2794 GeV
$\eta_B$	0.55	$\tilde{m}_t(m_t)$	170 GeV
$\mu_B$	2.5 GeV	$m_b(\mu_B)$	4.88 GeV
$\alpha_s(\mu_B)$	0.276	$\mu_{\text{SUSY}}$	$\sqrt{\tilde{m}m_{\tilde{g}}}$

obtain  $B$  mass scale values. The renormalization group running of these Wilson coefficients including leading order QCD corrections is given in [23]. Since  $B_d^0-\bar{B}_d^0$  mixing is a  $\Delta B = 2$  process, we need a power of  $\delta$  in each of the internal squark lines to change flavor. There are altogether six combinations:  $\delta_{LL}^2$ ,  $\delta_{RR}^2$ ,  $\delta_{LL}\delta_{RR}$ ,  $\delta_{LR}^2$ ,  $\delta_{RL}^2$  and  $\delta_{LR}\delta_{RL}$ , as is evident from (5).

To obtain  $\Delta m_{B_d}$ , we use  $\Delta m_{B_d} = 2|M_{12}^B|$ , where

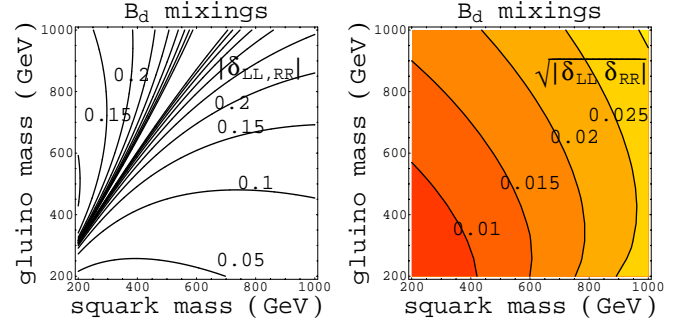
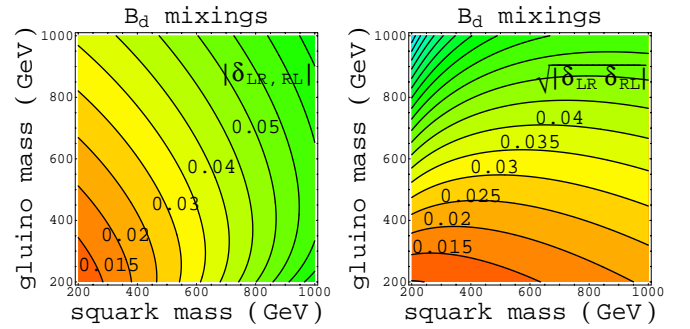
$$\begin{aligned} M_{12}^B &\equiv |M_{12}^B|e^{2i\phi_{B_d}} \\ &= |M_{12}^{\text{SM}}|e^{2i\phi_1} + |M_{12}^{\text{SUSY}}|e^{i\phi_{\text{SUSY}}}, \end{aligned} \quad (8)$$

and

$$\begin{aligned} M_{12}^{\text{SM}} &= 0.33 \left( \frac{f_{B_d}\sqrt{\hat{B}_{B_d}}}{230 \text{ MeV}} \right)^2 \left( \frac{\tilde{m}_t(m_t)}{170 \text{ GeV}} \right)^{1.52} \\ &\times \left( \frac{\eta_B}{0.55} \right) \left( \frac{|V_{td}|}{8.8 \times 10^{-3}} \right)^2 e^{2i\phi_1} \text{ ps}^{-1}, \end{aligned} \quad (9)$$

where  $M_{12}^{\text{SM}}$  is the SM contribution; its value is well known [24]. The vacuum insertion matrix elements of  $\mathcal{O}_i$  are given in [18]. These matrix elements are modified by bag factors to include non-factorizable effects. For simplicity, we assume the bag factors for matrix elements of  $\mathcal{O}_{2-5}$  to be equal to  $\hat{B}_{B_d}$ , which is calculated for  $\mathcal{O}_1$ . In the subsequent numerical analysis, we take  $f_{B_d}\hat{B}_{B_d}^{1/2} = (230 \pm 40)$  MeV [26]. For the CKM matrix elements, we take  $|V_{ub}/\lambda V_{cb}| = 0.41$  and  $\phi_3 = 65^\circ$ , hence  $|V_{td}| \times 10^3 = 8.0$  to get  $\Delta m_{B_d}^{\text{SM}} \sim 0.54 \text{ ps}^{-1}$ , which is close to the experimental value of  $\Delta m_{B_d} = 0.484 \pm 0.010 \text{ ps}^{-1}$  [25]. We summarize the input parameters used in Table 1.

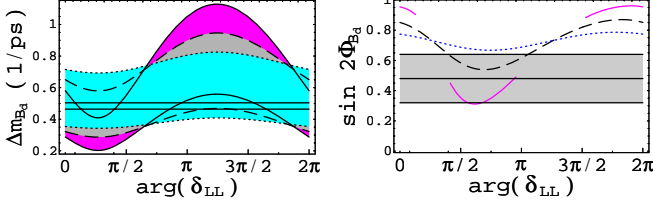
In Figs. 1 and 2, we show estimated limits of all six  $|\delta\delta|^{1/2}$ s over the parameter space of sub-TeV gluino and squarks. The limits are taken such that [8] the SUSY contribution to  $B_d$  mixing matrix element,  $|M_{12}|$ , is comparable with the SM result; hence large interference effects could in principle occur that can give a low  $a_{J/\psi K_S}$ . Note that by assuming the same bag factor for  $\mathcal{O}_i$ , the uncertainty on  $f_{B_d}\hat{B}_{B_d}^{1/2}$  does not show up in these figures. Squark mixing angles that are much larger than those shown would give too large a contribution to  $B_d$  mixing and would require fine tuning to satisfy the experimental result. For mixing angles that are much smaller than those shown, they will not be able to generate a large enough interference effect to reduce the asymmetry. Therefore, the limits shown in these figures may serve as


**Fig. 1a,b.** Limits on  $\delta_{LL,RR}$  and  $\delta_{LL}\delta_{RR}$  obtained by assuming  $|M_{12}^{\text{SUSY}}| < |M_{12}^{\text{SM}}|$  in  $B_d$  mixing

**Fig. 2a,b.** Limits on  $\delta_{LR,RL}$  and  $\delta_{LR}\delta_{RL}$  obtained by assuming  $|M_{12}^{\text{SUSY}}| < |M_{12}^{\text{SM}}|$  in  $B_d$  mixing

upper limits from the  $\Delta m_{B_d}$  constraint on one hand, and serve as roughly the required values to give an impact on  $a_{J/\psi K_S}$ .

From Figs. 1 and 2 we see that the limits on  $|\delta_{LL}\delta_{RR}|^{1/2}$ ,  $|\delta_{LR,RL}|$  and  $|\delta_{LR}\delta_{RL}|^{1/2}$  are all of order few %, with  $|\delta_{LL}\delta_{RR}|^{1/2}$  as the most sensitive source for  $B_d$  mixing. This can be understood from (5), where  $|\delta_{LL}\delta_{RR}|^{1/2}$  in  $C_4$  has the largest  $N_c$  factor, while there is also RG enhancement [23]. Furthermore, we see from (5) that the dominant  $\delta_{LL}\delta_{RR}$  and  $\delta_{LR,RL}^2$  terms are proportional to  $x_{\tilde{g}\tilde{q}}f_6(x_{\tilde{g}\tilde{q}})/\tilde{m}^2$ , while dominant  $\delta_{LR}\delta_{RL}$  term is proportional to  $f_6(x_{\tilde{g}\tilde{q}})/\tilde{m}^2$ . Therefore, the bounds on  $|\delta_{LL}\delta_{RR}|^{1/2}$  and  $|\delta_{LR,RL}|$  are roughly proportional to  $(\tilde{m}^2/[x_{\tilde{g}\tilde{q}}f_6(x_{\tilde{g}\tilde{q}})])^{1/2}$ , while the bound on  $|\delta_{LR}\delta_{RL}|^{1/2}$  is roughly proportional to  $(\tilde{m}^2/|f_6(x_{\tilde{g}\tilde{q}})|)^{1/2}$ , such that Figs. 1b and 2a show a similar behavior that is different from Fig. 2b.

The order of magnitude of these figures can be understood by a simple dimensional analysis. Comparing the SUSY versus SM box diagram contributions, we find  $\delta \lesssim V_{tb}V_{td}^*(\alpha_W/\alpha_S)(m_t\tilde{m}/M_W^2)(1/\sqrt{N_c}) \lesssim 2.8 \times 10^{-2}(\tilde{m}/500 \text{ GeV})$ , which is very close to the limits on  $|\delta_{LR,RL}|$ ,  $|\delta_{LR}\delta_{RL}|^{1/2}$  and  $|\delta_{LL}\delta_{RR}|^{1/2}$  from Figs. 1b and 2. However, the limit on  $|\delta_{LL,RR}|$  as shown in Fig. 1a are of the order of a few 10% and do not obey this estimation. This rather different behavior is because of the possible cancellation between  $x_{\tilde{g}\tilde{q}}f_6(x_{\tilde{g}\tilde{q}})$  and  $\tilde{f}_6(x_{\tilde{g}\tilde{q}})$  in  $C_1(\tilde{C}_1)$ , which can weaken the bounds. A total cancellation is reflected in the valley along  $x_{\tilde{g},\tilde{q}} \sim 2.43$  where  $|\delta_{LL,RR}|$  is not con-



**Fig. 3a,b.** Dotted, dashed and solid lines correspond to **a**  $\Delta m_{B_d}$ , **b**  $\sin 2\Phi_{B_d}$ , induced by  $\delta_{RR} = |\delta_{LL}| = (0.3, 0.5, 0.7) \times 0.013$  with  $\tilde{m}, m_{\tilde{g}} = 500, 400$  GeV, respectively. The horizontal band in the left (right) figure is  $2\sigma(1\sigma)$  experimental range

strained by  $|M_{12}^{\text{SUSY}}| \sim |M_{12}^{\text{SM}}|$ . From (5) and (7), we see that  $C_1$  is dominated by  $x_{\tilde{g}\tilde{q}} \tilde{f}_6(x_{\tilde{g}\tilde{q}})$  for  $x_{\tilde{g}\tilde{q}} \gg 1$  and dominated by  $\tilde{f}_6(x_{\tilde{g}\tilde{q}})$  for  $x_{\tilde{g}\tilde{q}} \ll 1$ . Therefore, apart from the distortion due to the cancellation discussed earlier, the upper left part of Fig. 1a is similar to Figs. 1b and 2a, while the lower right part is similar to Fig. 2b. Note that whenever we obtain a bound that is greater than  $O(1)$  in the squark mixing angle  $\delta$ , it should be interpreted as signaling the need of a large squark mass splitting which invalidates the approximation of (4).

It is clear that, to obtain a low  $a_{J/\psi K_S}$ , we need a suitable SUSY phase to have destructive interference with SM. But the minimum requirement is that the SUSY amplitude should be large enough to allow for such an interference effect. As shown in this section, it is possible for SUSY models to give  $B_d$  mixing that is comparable to the SM result and hence lead to a large interference effect. Mixing angles of a few% in left–right squark mixings or few% to few 10% in left–left, right–right squark mixings are sufficient to achieve this. The case with both left–left and right–right mixings ( $\delta_{LL}\delta_{RR}$ ) is most sensitive to the mixing angles, while left–left or right–right mixing alone are the least sensitive, and could even be totally insensitive for a fine-tuned parameter space near  $x_{\tilde{g}\tilde{q}} \equiv m_{\tilde{g}}^2/\tilde{m}^2 \sim 2.43$ .

For illustration, we pick a point from Figs. 1 and 2, say  $(\tilde{m}, m_{\tilde{g}}) = (500, 400)$  GeV, and show the SUSY effects on  $B_d$  mixing. For the LL–RR mixing case, the bound is 0.013, as shown in Figure 1b. We show in Fig. 3  $\Delta m_{B_d}$  and  $\sin 2\Phi_{B_d}$ , induced by  $\delta_{RR} = |\delta_{LL}| = (30\%, 50\%, 70\%) \times 0.013$ , versus  $\arg(\delta_{LL})$ , respectively. The  $|\delta_{LL}\delta_{RR}|^{1/2}$  are (30%, 50%, 70%) of the bound shown in Fig. 1b for the particular  $\tilde{m}, m_{\tilde{g}}$ . Larger oscillating amplitudes in the figures correspond to larger  $\delta_{LL,RR}$ . Similar results will be obtained by using (30%, 50%, 70%) of the corresponding bounds of the other points on the  $(\tilde{m}, m_{\tilde{g}})$  plane, shown in Figs. 1 and 2. The horizontal band in the left (right) figure is the  $2\sigma(1\sigma)$  experimental range. The uncertainty of the predicted  $\Delta m_{B_d}$  is due to the  $\sim 17\%$  uncertainty of  $f_{B_d} \hat{B}_d^{1/2}$  as shown in Table 1. This factor does not enter  $\arg(M_{12}^B)$ , and thus  $\sin 2\Phi_{B_d}$  shown in Fig. 3b, as we assume all bag factors for different  $\mathcal{O}_i$  to be the same. By using a  $\delta$  at 30% of the bound value,  $B_d$  mixing does not differ much from the SM prediction, while for the 50% case, it starts to show an interesting deviation with  $\sin 2\Phi_{B_d}$  as low as 0.53. Note that the SM gives  $\sin 2\phi_1 = 0.73$  by

using our input parameters. For a larger  $\delta$ , such as 70% of the bound, it can further lower  $\sin 2\Phi_{B_d}$  to 0.3. Although in this case not all  $\arg(\delta_{LL})$  are allowed, due to the  $\Delta m_{B_d}$  constraint, we still have plenty of allowed region for this phase. From these figures, we see that by using 50%–70% of the  $\delta$  bounds, a low  $\sin 2\Phi_{B_d}$  can easily be obtained.

### 3 $B \rightarrow \pi\pi$ and $\rho\gamma$ decays in SUSY models

The effective Hamiltonian for charmless  $b \rightarrow d$  decays is

$$H_{\text{eff}} = \frac{4G_F}{\sqrt{2}} \left[ V_{ub}V_{ud}^*(c_1 O_1 + c_2 O_2) - V_{tb}V_{td}^* \sum_{i=3}^{10} c_i O_i - V_{tb}V_{td}^*(C_g \tilde{O}_g + C'_g \tilde{O}'_g) \right], \quad (10)$$

where, as a matter of convention, we factor out a CKM factor  $V_{tb}V_{td}^*$  even for the SUSY contributions. The operators are defined by

$$\begin{aligned} O_1 &= \bar{u}\gamma_\mu L b \bar{d}\gamma^\mu L u, \\ O_2 &= \bar{u}_\alpha \gamma_\mu L b_\beta \bar{d}_\beta \gamma^\mu L u_\alpha, \\ O_{3(5)} &= \bar{d}\gamma_\mu L b \bar{q}\gamma^\mu L(R)q, \\ O_{4(6)} &= \bar{d}_\alpha \gamma_\mu L b_\beta \bar{q}_\beta \gamma^\mu L(R)q_\alpha, \\ O_{7(9)} &= \frac{3}{2} \bar{d}\gamma_\mu L b Q q \bar{q}\gamma^\mu R(L)q, \\ O_{8(10)} &= \frac{3}{2} \bar{d}_\alpha \gamma_\mu L b_\beta Q q \bar{q}_\beta \gamma^\mu R(L)q_\alpha, \\ \tilde{O}_g^{(\prime)} &= \frac{\alpha_s}{4\pi} \bar{d} i \sigma_{\mu\nu} T^a \frac{2m_b q^\nu}{q^2} R(L) b \bar{q} \gamma^\mu T^a q, \end{aligned} \quad (11)$$

where  $L, R = (1 \mp \gamma_5)/2$ ,  $\tilde{O}_g^{(\prime)}$  arises from the dimension 5 color dipole operator, and  $q = p_b - p_d$ . Note that with new physics, one may also have chiral conjugates of  $O_{1-10}$  with Wilson coefficients defined by  $c'_{1-10}$ . The Wilson coefficient  $C'_g$  and the color dipole operators are defined in the effective Hamiltonian for  $b \rightarrow d\gamma, dg$  transitions,

$$H_{\text{eff}} = -\frac{V_{tb}V_{td}^* m_b G_F}{4\sqrt{2}\pi^2} \{ e\bar{d} [C_\gamma R + C'_\gamma L] \sigma_{\mu\nu} F^{\mu\nu} b + g\bar{d} [C_g R + C'_g L] \sigma_{\mu\nu} T^a G_a^{\mu\nu} b \}, \quad (12)$$

where we have neglected  $m_d$ ,  $C_{\gamma,g} = C_{\gamma,g}^{\text{SM}} + C_{\gamma,g}^{\text{new}}$  are the sum of the SM and new physics contributions, while the  $C'_{\gamma,g}$  come purely from new physics.

For  $\bar{B}^0 \rightarrow \pi^+\pi^-$ , using the factorization approach, we find [14, 27, 28]

$$\begin{aligned} iM &= -i \frac{G_F}{\sqrt{2}} f_\pi F_0^{B \rightarrow \pi} (m_\pi^2) (m_B^2 - m_\pi^2) \{ V_{ub}V_{ud}^* a_1 \\ &\quad - V_{tb}V_{td}^* [\Delta a_4 + \Delta a_{10} + (\Delta a_6 + \Delta a_8) R \\ &\quad + \frac{\alpha_s}{4\pi} \frac{2m_b^2}{q^2} \tilde{S}_{\pi\pi} (C_g - C'_g)] \}, \end{aligned} \quad (13)$$

$$R = \frac{2m_\pi^2}{(m_b - m_u)(m_u + m_d)}, \quad (14)$$

**Table 2.** The input parameters used in this section

Parameter	Value	Parameter	Value
$F_0(0)$	$0.30 \pm 0.04$	$f_\pi$	133 MeV
$m_\pi$	140 MeV	$\tau_B$	1.548 ps
$m_u(\mu_B)$	2 MeV	$m_d(\mu_B)$	4 MeV
$m_{u,d}^{\text{const.}}$	0.2 GeV	$m_s^{\text{const.}}$	0.5 GeV
$m_c^{\text{const.}}$	1.5 GeV	$\langle q^2 \rangle$	$m_b^2/3$

$$\begin{aligned} \tilde{S}_{\pi\pi} = & -\frac{N_c^2 - 1}{2N_c^2} \left\{ (1 + R) - R \frac{m_B^2(m_b - m_u)}{2m_b(m_B^2 - m_\pi^2)} \right. \\ & \times \left( \frac{3f^+(m_\pi^2)}{2F_0(m_\pi^2)} + \frac{f^-(m_\pi^2)}{2F_0(m_\pi^2)} \right) + \frac{m_B^2}{2m_b(m_b - m_u)} \\ & \left. - \frac{4m_b h(m_\pi^2)}{F_0(m_\pi^2)} \frac{m_B^2(m_B^2 - 4m_\pi^2)}{8m_b^2(m_B^2 - m_\pi^2)} \right\}, \end{aligned} \quad (15)$$

where  $\Delta a_i$  is defined as  $a_i - a'_i$  with  $a_i^{(\prime)} \equiv c_i^{(\prime)} + c_{i\mp 1}^{(\prime)}/N_c$ , for even (odd)  $i$ . Using input parameters shown in Table 2, the chiral factor  $R = 1.33$ . The expression for  $\tilde{S}_{\pi\pi}$  is somewhat different from the one given in [27] because of the treatment of  $q^\nu$  in  $\tilde{O}_g^{(\prime)}$ . We have used

$$\begin{aligned} \bar{d}\sigma_{\mu\nu}q^\nu T^a R b \bar{q} \gamma^\mu T^a q \\ = -(\bar{d}\gamma_\mu \not{p}_b T^a R b + \bar{d} \not{p}_d \gamma_\mu T^a R b)(\bar{q} \gamma^\mu T^a q) \\ + \bar{d} T^a R b p_{b\mu} [\not{q}(2 \not{p}_b - \not{q}) \gamma^\mu T^a q], \end{aligned} \quad (16)$$

where the  $\not{q}$  term can be dropped because of current conservation. By using heavy quark symmetry,  $p_b \rightarrow p_B$ , it is then straightforward to use the factorization approach to obtain  $\tilde{S}_{\pi\pi}$  as given in (15). For the form factors involved, we have the relations [27]  $f^+(m_\pi^2) = F_1(m_\pi^2)$ ,  $f^-(m_\pi^2) = (m_B^2/m_\pi^2 - 1)[F_0(m_\pi^2) - F_1(m_\pi^2)]$  and  $4m_b h(m_\pi^2) = f_+(m_\pi^2) - f^-(m_\pi^2)$ . Using  $F_0(0) = F_1(0) = 0.30 \pm 0.04$  and the monopole form factors for  $F_{0,1}$ , with pole masses given in [14], it is easy to show that  $f^+(m_\pi^2)/F_0(m_\pi^2) \sim 1$ ,  $f^-(m_\pi^2)/F_0(m_\pi^2) \sim 0$ , and  $4m_b h(m_\pi^2)/F_0(m_\pi^2) \sim 1$ . Therefore,

$$\tilde{S}_{\pi\pi} \simeq -\frac{N_c^2 - 1}{2N_c^2} \left( \frac{11}{8} + \frac{R}{4} \right) \simeq -0.76, \quad (17)$$

which is not far from the value of  $-0.80$  computed from (15), and also close to the value given in [28]. Note that it is insensitive to  $N_c$  and the chiral factor  $R$ . The opposite sign between  $(a_i, C_g)$  and  $(a'_i, C'_g)$  can easily be understood by using a parity transformation. We note that the color dipole term is sensitive to  $\langle q^2 \rangle$ , which is usually taken to be between  $m_b^2/4$  and  $m_b^2/2$ . We use  $\langle q^2 \rangle \sim m_b^2/3^1$ . The  $q^2$  dependence will affect the color dipole contribution by  $\pm 33\%$  at amplitude level.

Using the input parameters shown in Tables 1 and 2 and following the approach in [14], we obtained the numerical values of  $a_i$ s in SM, as shown in Table 3. In SM,  $C_g^{\text{SM}} = -0.15$ , while  $C_g^{\text{SM}}$  is highly suppressed by the

<sup>1</sup> When comparing this to the QCD factorization approach, we may use effectively  $\langle q^2 \rangle \sim m_b^2/3 - m_b^2/2.4$  in the color dipole contribution [29]

V–A nature of the weak interaction and the smallness of  $m_d$ . The  $C_g^{\text{SM}}$  contribution is about 3% of the tree amplitude. In the factorization approximation, the SM gives  $\text{Br}(\bar{B}^0 \rightarrow \pi^+\pi^-) \sim 10 \times 10^{-6}$ , with  $\sim 3.3\%$  asymmetry, as defined by

$$a_{\pi^+\pi^-} = \frac{\text{Br}(B^0 \rightarrow \pi^+\pi^-) - \text{Br}(\bar{B}^0 \rightarrow \pi^+\pi^-)}{\text{Br}(B^0 \rightarrow \pi^+\pi^-) + \text{Br}(\bar{B}^0 \rightarrow \pi^+\pi^-)}. \quad (18)$$

Since this process is tree dominant, we need a large contribution if this rate is to be reduced by a new physics contribution.

In SUSY models, we can have gluino, neutralino, chargino and charged Higgs exchange contributions to  $B \rightarrow \pi\pi$ . Because of  $N_c$  enhancement and different sensitivities of photonic versus gluonic penguins [30], and since one does not suffer from the  $\text{Br}(B \rightarrow X_s \gamma)$  constraint, we see that gluino exchange gives a dominant and interesting contribution to  $B \rightarrow \pi\pi$  as compared to other superparticles. There are two types of diagrams: the gluino box and the gluino penguin. The former as well as the  $F_1$  term (the quark chirality conserving vertex term) of the latter contribute to  $a_i$ , and only depend on one power of  $\delta_{LL,RR}$ . The  $F_2$  term (the quark chirality flipped vertex term) of the gluino penguin contributes through  $C_g^{(\prime)}$  with all types of squark mixings. We use similar formulas as in [18] for the SUSY contribution and those of [24,31] for the RG running.

The gluino box and  $F_1$  gluino penguin give

$$\begin{aligned} c_3(M_{\text{SUSY}}) &= \frac{\alpha_s^2 \delta_{LL}}{2\sqrt{2}G_f V_{tb} V_{td}^* \tilde{m}^2} \left[ -\frac{1}{N_c^2} B_1(x_{\tilde{g}\tilde{q}}) \right. \\ &\quad \left. - \frac{1}{2} \left( 1 + \frac{1}{N_c^2} \right) B_2(x_{\tilde{g}\tilde{q}}) - \frac{1}{N_c} P(x_{\tilde{g}\tilde{q}}) \right], \\ c_4(M_{\text{SUSY}}) &= \frac{\alpha_s^2 \delta_{LL}}{2\sqrt{2}G_f V_{tb} V_{td}^* \tilde{m}^2} \quad (19) \\ &\quad \times \left[ \left( -N_c + \frac{2}{N_c} \right) B_1(x_{\tilde{g}\tilde{q}}) + \frac{1}{N_c} B_2(x_{\tilde{g}\tilde{q}}) + P(x_{\tilde{g}\tilde{q}}) \right], \\ c_5(M_{\text{SUSY}}) &= \frac{\alpha_s^2 \delta_{LL}}{2\sqrt{2}G_f V_{tb} V_{td}^* \tilde{m}^2} \\ &\quad \times \left[ \left( 1 + \frac{1}{N_c^2} \right) B_1(x_{\tilde{g}\tilde{q}}) + \frac{1}{2N_c^2} B_2(x_{\tilde{g}\tilde{q}}) - \frac{1}{N_c} P(x_{\tilde{g}\tilde{q}}) \right], \\ c_6(M_{\text{SUSY}}) &= \frac{\alpha_s^2 \delta_{LL}}{2\sqrt{2}G_f V_{tb} V_{td}^* \tilde{m}^2} \\ &\quad \times \left[ -\frac{2}{N_c} B_1(x_{\tilde{g}\tilde{q}}) + \frac{1}{2} \left( N_c - \frac{2}{N_c} \right) B_2(x_{\tilde{g}\tilde{q}}) + P(x_{\tilde{g}\tilde{q}}) \right], \end{aligned}$$

where  $c'_i$  are obtained from  $c_i$  by replacing  $L \leftrightarrow R$ , the  $B_i(x)$  are from the gluino box, the  $P(x) \equiv [C_2(G)/2 - C_2(R)]P_1(x) + C_2(G)P_2(x)/2$  are from the  $F_1$  term, and  $C_2(G) = N_c$  and  $C_2(R) = (N_c^2 - 1)/2N_c$  are Casimirs. The  $P_{1(2)}(x_{\tilde{g}\tilde{q}})$  term corresponds to a gluon attached to squark (gluino) line. The gluino box contribution to  $c_{3,4(5,6)}$  are due to  $\tilde{d}_L-\tilde{b}_L$  mixings in one of the squark line, while the other squark line is  $\tilde{q}_{L(R)}$ . The leading terms in  $N_c$  are the  $B_1(x)$  and  $B_2(x)$  terms of  $c_4$  and  $c_6$ , respectively. Explicit

**Table 3.** The  $a_i$ s in SM for  $b \rightarrow d$  and  $\bar{b} \rightarrow \bar{d}$  for  $\phi_3 = 65^\circ$ 

$a_i$	$b \rightarrow d$	$\bar{b} \rightarrow \bar{d}$	$a_i$	$b \rightarrow d$	$\bar{b} \rightarrow \bar{d}$
$a_1$	1.0463	1.0463	$a_6$	$-0.0473 + 0.0091i$	$-0.0674 + 0.0029i$
$a_2$	0.0502	0.0502	$a_7$	0.0002	-0.0000
$a_3$	0.0049	0.0049	$a_8$	0.0005	0.0004
$a_4$	$-0.0337 + 0.0091i$	$-0.0538 + 0.0029i$	$a_9$	-0.0093	-0.0095
$a_5$	-0.0044	-0.0044	$a_{10}$	-0.0013	-0.0014

forms of  $B_i(x), P_i(x)$  can be found in [18]. They can be expressed by

$$[-4B_1(x_{\bar{g}\bar{q}}), B_2(x_{\bar{g}\bar{q}})] = \tilde{m}^4 \frac{\partial}{\partial \tilde{m}^2} \int_0^\infty dk^2 \times \left\{ \frac{k^2}{(k^2 + m_{\bar{g}}^2)^2 (k^2 + \tilde{m}^2)} \frac{[k^2, m_{\bar{g}}^2]}{(k^2 + \tilde{m}^2)} \right\} \Bigg|_{\tilde{m}' \rightarrow \tilde{m}}, \quad (20)$$

$$6[P_1(x_{\bar{g}\bar{q}}), -P_2(x_{\bar{g}\bar{q}})] = \tilde{m}^4 \frac{\partial}{\partial \tilde{m}^2} \int_0^\infty dk^2 \times \frac{k^4}{(k^2 + m_{\bar{g}}^2)(k^2 + \tilde{m}^2)} \left[ \frac{k^2}{(k^2 + \tilde{m}^2)^3}, \frac{2k^2 + 3m_{\bar{g}}^2}{(k^2 + m_{\bar{g}}^2)^3} \right]. \quad (21)$$

Note that  $B_1(x), P_2(x)$  are always positive, while  $B_2(x), P_1(x)$  are always negative. It is useful to give the asymptotic form of these functions:

$$\begin{aligned} & [B_1(x), B_2(x), P(x)] \\ &= \frac{1}{4} \begin{cases} [\ln x/x^2, -2/x, -1/(9x)], & x \gg 1, \\ [1/12, -1/3, 8/45], & x = 1, \\ [1/2, 4x \ln x, -2 \ln x], & x \ll 1. \end{cases} \end{aligned} \quad (22)$$

The gluonic and photonic penguins are closely related. The formulas for  $C_\gamma^{(l)}$  and  $C_g^{(l)}$  from gluino exchange are

$$C_\gamma = \frac{\pi\alpha_s}{\sqrt{2}G_F V_{tb}V_{td}^*} \frac{Q_d 2C_2(R)}{\tilde{m}^2} \times \left\{ \delta_{LL} g_2(x_{\bar{g}\bar{q}}) - \frac{m_{\bar{g}}}{m_b} \delta_{LR} g_4(x_{\bar{g}\bar{q}}) \right\}, \quad (23)$$

$$C_g = \frac{\pi\alpha_s}{\sqrt{2}G_F \tilde{m}^2 V_{tb}V_{td}^*} \{ \delta_{LL} ([2C_2(R) - C_2(G)] g_2(x_{\bar{g}\bar{q}}) - C_2(G) g_1(x_{\bar{g}\bar{q}})) + \frac{m_{\bar{g}}}{m_b} \delta_{LR} ([C_2(G) - 2C_2(R)] g_4(x_{\bar{g}\bar{q}}) + C_2(G) g_3(x_{\bar{g}\bar{q}})) \}, \quad (24)$$

with the chirality partners  $C'_{\gamma,g}$  obtainable by interchanging  $L \leftrightarrow R$  in the  $\delta$ 's,  $Q_d$  is the electric charge of the down type quarks and the functions  $g_i(x_{\bar{g}\bar{q}}) = -\tilde{m}^4 (\partial/\partial \tilde{m}^2) [F_i(x_{\bar{g}\bar{q}})/\tilde{m}^2]$ , where  $F_i(x)$  are given in [19], and can be expressed in terms of loop integrals:

$$\begin{aligned} & [F_1(x_{\bar{g}\bar{q}}), F_2(x_{\bar{g}\bar{q}}), F_2(x_{\bar{g}\bar{q}}), F_3(x_{\bar{g}\bar{q}}), F_4(x_{\bar{g}\bar{q}})] \\ &= \tilde{m}^2 \int_0^\infty dk^2 \frac{k^2}{(k^2 + m_{\bar{g}}^2)(k^2 + \tilde{m}^2)} \left[ \frac{k^2 m_{\bar{g}}^2}{2(k^2 + m_{\bar{g}}^2)^3}, \right. \end{aligned}$$

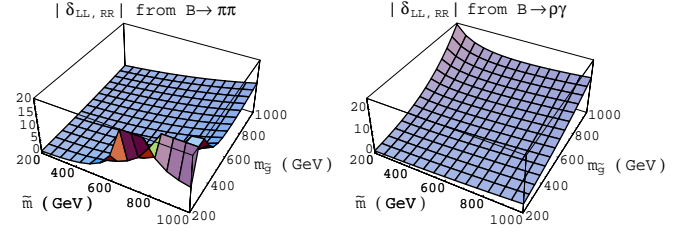


**Fig. 4a,b.** Lower and upper limits on squark mixing angles  $\delta_{LL,RR}$  obtained by **a**  $\text{Br}^{\text{SUSY}}(\pi^+\pi^-)/\text{Br}^{\text{SM}}(\pi^+\pi^-) > 10\%$ , **b**  $\text{Br}^{\text{SUSY}}(\rho^0\gamma)/\text{Br}^{\text{SM}}(\rho^0\gamma) < 4$ , respectively

$$\left[ \frac{k^2 \tilde{m}^2}{2(k^2 + \tilde{m}^2)^3}, \frac{k^2}{(k^2 + m_{\bar{g}}^2)^2}, \frac{\tilde{m}^2}{(k^2 + \tilde{m}^2)^2} \right]. \quad (25)$$

For future use, we give the asymptotic behavior of  $g_i(x_{\bar{g}\bar{q}})$ ,

$$\begin{aligned} & -6[g_1(x), g_2(x), g_3(x), g_4(x)] \\ &= \begin{cases} [1, 3 \ln x, 3, 6 \ln x]/x^2, & \text{for } x \gg 1, \\ [1/10, 3/20, 1/2, 1/2], & \text{for } x = 1, \\ [1, 1/2, -6 \ln x, 1], & \text{for } x \ll 1. \end{cases} \end{aligned} \quad (26)$$

From (23)–(25), it is clear that  $g_{2,4}(x_{\bar{g}\bar{q}})$  correspond to photon and gluon attached to the internal squark line, while  $g_{1,3}(x_{\bar{g}\bar{q}})$  correspond to the opposite case but only with the gluon attachment. Note that in the large  $N_c$  limit,  $C_2(G), 2C_2(R) \rightarrow N_c$ , while  $[2C_2(R) - C_2(G)] \rightarrow \mathcal{O}(1/N_c)$  is suppressed. One always has an  $N_c$  factor in  $C_\gamma^{(l)}$ , while for  $C_g^{(l)}$ , one only has the  $N_c$  factor when a gluon attaches to the internal gluino line, which can be easily understood by using 't Hooft's double line notation. This is also true for the  $F_1$  vertex term. However, the chiral enhancement factor  $m_{\bar{g}}/m_b$  accompanying  $\delta_{LR,RL}$  is a unique feature of the  $F_2$  term. The mechanism is generic and has been discussed in [32], but SUSY with LR squark mixings gives a beautiful example [33].

For direct destructive interference to cut down by half the predicted SM rate, one needs the SUSY amplitude to be 30% of the SM amplitude. This will be the minimum requirement on the SUSY contribution. In Figs. 4a and 5a we show limits on  $|\delta_{LL,RR}|$  and  $|\delta_{LR,RL}|$ , respectively. We require the SUSY contribution alone to give 10% of  $\text{Br}^{\text{SM}}(B \rightarrow \pi\pi)$ , corresponding to  $\sim 30\%$  in amplitude. If we change the required rate contribution by a factor  $\kappa$ , the values shown in the plots scale by a factor  $\kappa^{1/2}$ . From Fig. 4a, we see that the decay rate is insensitive to left–left

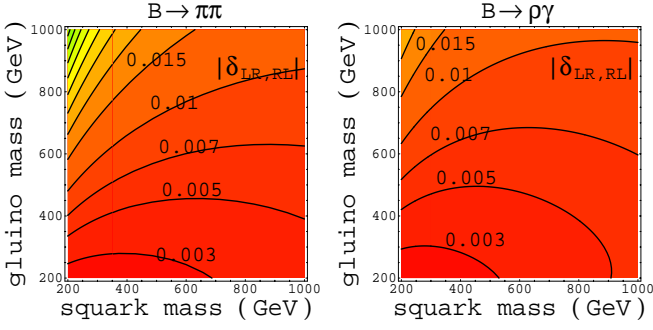


**Fig. 5a,b.** Lower and upper limits on squark mixing angles  $\delta_{LR,RL}$  obtained by **a**  $\text{Br}^{\text{SUSY}}(\pi^+\pi^-)/\text{Br}^{\text{SM}}(\pi^+\pi^-) > 10\%$ , **b**  $\text{Br}^{\text{SUSY}}(\rho^0\gamma)/\text{Br}^{\text{SM}}(\rho^0\gamma) < 4$ , respectively

and right–right squark mixings, which means that gluino box and  $\delta_{LL,RR}$  related gluino penguins do not give large contributions.

The SUSY contribution from the gluino box and the  $F_1$  term is dominated by  $B_{1,2}(x_{\tilde{g}\tilde{q}})$ ,  $P(x_{\tilde{g}\tilde{q}})$  and  $g_1(x_{\tilde{g}\tilde{q}})$ . For  $\tilde{m} \ll m_{\tilde{g}}$ ,  $B_2(x_{\tilde{g}\tilde{q}})$  is dominant and contributes through  $c_6$ , which is from the gluino box containing  $\tilde{d}_L\text{--}\tilde{b}_L$  and  $\tilde{q}_R$  squark lines. For  $m_{\tilde{g}} \ll \tilde{m}$ ,  $P(x_{\tilde{g}\tilde{q}})$  is dominant and contributes through  $c_{4,6}$ . However, from (13), (19), (22), (24) and (26), we see that this  $F_1$  term always receives a cancellation from  $B_1(x_{\tilde{g}\tilde{q}})$  and  $g_1(x_{\tilde{g}\tilde{q}})$ , which are not too small in this region. Therefore the rise in the lower right corner of Fig. 4a shows insensitivity to  $\delta_{LL,RR}$  as a consequence of this cancellation effect.

In Fig. 5a, we show the required  $|\delta_{LR,RL}|$  to produce a large enough SUSY contribution in  $B \rightarrow \pi\pi$  decay. Note that in (24), we use a running  $m_b(\mu_{\text{SUSY}})$ . For most of the parameter space a less than 2% mixing angle in left–right mixing is enough to generate such a large SUSY contribution. The sensitivity is greatly enhanced from the previous case due to the chiral enhancement factor  $m_{\tilde{g}}/m_b$ . Note that there is nothing peculiar about chiral enhancement. It only reflects the chiral suppression of  $C_{g,\gamma}$  in the SM due to the V–A nature of the weak interaction, which need not be obeyed by interactions beyond the SM.

For the left–right mixing case as shown in Fig. 5a, we see that the SUSY contribution is larger for squark mass greater than the gluino mass and vice versa. For the case of a heavy squark and a light gluino ( $x_{\tilde{g}\tilde{q}} \equiv m_{\tilde{g}}^2/\tilde{m}^2 < 1$ ), the gluon preferably radiates off the gluino rather than the squark line, as is clear from the behavior of  $g_3(x_{\tilde{g}\tilde{q}})$  in (24)–(26). Note that this is the one with  $N_c$  enhancement and therefore gives a larger contribution compared to  $\tilde{m} < m_{\tilde{g}}$  case, where the dominant diagrams do not have  $N_c$  enhancement. The SUSY contribution is dominated by  $\delta_{LR,RL}m_{\tilde{g}}g_3(x_{\tilde{g}\tilde{q}})/(m_b\tilde{m}^2)$ . For  $\tilde{m} \ll m_{\tilde{g}}$ , as shown in (26), this term becomes  $\delta_{LR,RL}\tilde{m}^2/(2m_{\tilde{g}}^3m_b)$  and is consistent with the sharp rise in the upper left corner of Fig. 5a. The SUSY contribution is small and insensitive to squark mixing angle in this region. This is a generic feature for gluino penguin contributions, as one can see from (26) that all  $g_i/\tilde{m}^2$  receive a  $\tilde{m}^2/m_{\tilde{g}}^4$  suppression factor in this region. In the reversed case of  $m_{\tilde{g}} \ll \tilde{m}$ , there is only  $1/\tilde{m}^2$

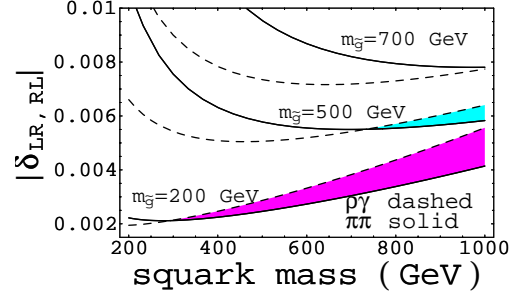


**Fig. 6.** Dashed [solid] lines are upper [lower] bounds on the squark mixing angles  $\delta_{LR,RL}$  obtained by  $\text{Br}^{\text{SUSY}}(\rho^0\gamma)/\text{Br}^{\text{SM}}(\rho^0\gamma) < 4$  [ $\text{Br}^{\text{SUSY}}(\pi^+\pi^-)/\text{Br}^{\text{SM}}(\pi^+\pi^-) > 10\%$ ] with  $m_{\tilde{g}} = 200, 500, 700$  GeV, respectively. Shaded regions are allowed parameter space

suppression, while the  $g_3(x_{\tilde{g}\tilde{q}})$  contribution receives  $\ln x_{\tilde{g}\tilde{q}}$  enhancement.

The gluino exchange induced photonic penguin is closely related to the gluonic penguin. For example, they have a similar chiral enhancement behavior as well as asymptotic behavior. Recently, the Belle Collaboration reported a 90% upper limit on  $\text{Br}(B^0 \rightarrow \rho^0\gamma) < 1.06 \times 10^{-5}$  [34], nominally  $\sim 5$  times the SM prediction, but a factor of 2 above their previous result reported at ICHEP2000 [35]. We require the decay rate due to the SUSY contribution alone to be smaller than 4 times the SM prediction. The bounds correspond to  $|C_{\gamma}^{(\prime)\text{SUSY}}| \sim 2|C_{\gamma}^{\text{SM}}|$ . Note that in the LR case, one may have cancellation between SM and SUSY  $C_{\gamma}$ . For a direct cancellation, the bounds on  $\delta_{LR}$  can be relaxed by 50%. In Fig. 4b and 5b, we show the limits on  $|\delta_{LL,RR}|$  and  $|\delta_{LR,RL}|$ , respectively. Similar to the  $B \rightarrow \pi\pi$  case, the decay rate is insensitive to  $|\delta_{LL,RR}|$ , but very sensitive to  $|\delta_{LR,RL}|$ , as expected. We also see a sharp rise in the upper left corners of Figs. 4b and 5b, which are similar to 5a and indicate that SUSY contributions are insensitive to the corresponding squark mixings in that region, as we have explained in the previous paragraph.

We note that in most of the parameter space shown in Fig. 5b, the  $|\delta_{LR,RL}|$  are constrained to be less than 2%. When compared to Fig. 5a, in most of the parameter space  $|\delta_{LR,RL}|$  impacts more on  $B \rightarrow \rho\gamma$  than  $B \rightarrow \pi\pi$ . This can easily be understood by noting that the former is a pure loop process while the latter is dominated by tree diagrams in SM. Therefore, it is easier for new physics to affect the former process.

It is quite interesting that, for the parameter space of  $\tilde{m} \sim 300\text{--}1000$  GeV and  $m_{\tilde{g}} \leq 700$  GeV, with mixing angle  $\sim 0.2\%\text{--}0.8\%$ , the model gives a sizable contribution to  $B \rightarrow \pi\pi$  decay that can account for the smallness of the rate, but still satisfy the  $B \rightarrow \rho\gamma$  constraint. As shown in Fig. 6, where the dashed (solid) lines correspond to upper (lower) limits on  $|\delta_{LR,RL}|$  from  $B \rightarrow \rho\gamma(\pi\pi)$ , with  $m_{\tilde{g}} = 200, 500, 700$  GeV, respectively. The shaded regions are the allowed parameter space for a given  $m_{\tilde{g}}$ . For  $m_{\tilde{g}} > 700$  GeV we need  $\tilde{m} > 1$  TeV to attain the allowed region, which is beyond the plot. In addition, one can also use a smaller  $\langle q^2 \rangle$ , such as  $m_{\tilde{g}}^2/4$ , to enhance

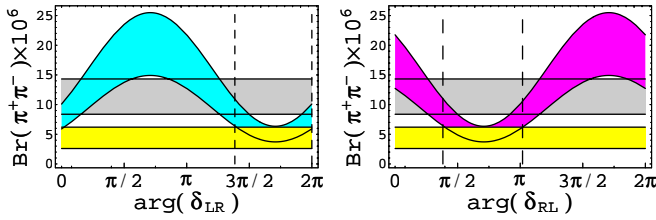


**Fig. 7a,b.**  $\text{Br}(B \rightarrow \pi\pi)$  obtained by using  $\tilde{m} = 800$  GeV,  $m_{\tilde{g}} = 200$  GeV, and **a**  $|\delta_{\text{LR}}| = 0.0035$ , **b**  $|\delta_{\text{RL}}| = 0.0035$ , respectively. The upper band corresponds to the SM prediction, while the lower band corresponds to the experimental result with  $2\sigma$  error range

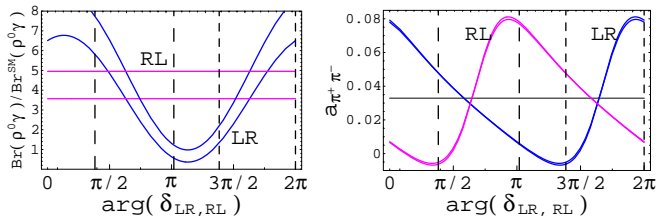


**Fig. 8. a** Upper (lower) lines correspond to  $\text{Br}(\rho^0\gamma) / \text{Br}^{\text{SM}}(\rho^0\gamma)$  with  $m_{\tilde{g}} = 200(500)$  GeV,  $\tilde{m} = 800(900)$  GeV,  $|\delta_{\text{LR,RL}}| = 0.0035(0.006)$ . **b** The asymmetry in  $B \rightarrow \pi^+\pi^-$  with the same parameter space as case **a**

the color dipole contribution and thus reduce the limit by 33% and enlarge the overlapping parameter space between Figs. 5a,b. The existence of this overlap region is closely related to the behavior of  $g_i(x_{\tilde{g}\tilde{q}})$ . From (23) and (24), it is clear that for left–right mixing,  $C'_\gamma \propto m_{\tilde{g}}/m_b g_4(x_{\tilde{g}\tilde{q}})$ , while  $C'_g \propto m_{\tilde{g}}/m_b g_3(x_{\tilde{g}\tilde{q}})$ . For  $x_{\tilde{g}\tilde{q}} \ll 1$ ,  $g_3(x_{\tilde{g}\tilde{q}})/g_4(x_{\tilde{g}\tilde{q}}) \rightarrow 6|\ln x_{\tilde{g}\tilde{q}}|$  can be rather sizable. Therefore, the gluino penguin can give a larger contribution in  $b \rightarrow d\gamma$  than in the  $b \rightarrow d\gamma$  process.

For illustration, we pick some points from Fig. 6 and study the impact of the SUSY contributions on  $\text{Br}(\pi^+\pi^-)$  and  $\text{Br}(\rho^0\gamma)$ . In Fig. 7, we show  $\text{Br}(\pi^+\pi^-)$  obtained by using  $m_{\tilde{g}} = 200$  GeV,  $\tilde{m} = 800$  GeV, and (a)  $|\delta_{\text{LR}}| = 0.0035$ ,  $\delta_{\text{RL}} = \delta_{\text{LL,RR}} = 0$ , (b)  $|\delta_{\text{RL}}| = 0.0035$ ,  $\delta_{\text{LR}} = \delta_{\text{LL,RR}} = 0$ , respectively. The upper band corresponds to the SM prediction, while the lower band corresponds to the averaged experimental result  $\text{Br}(\pi^+\pi^-) = 4.4 \pm 0.9$  with a  $2\sigma$  error range. With  $\arg(\delta_{\text{LR,RL}})$  within the dashed lines, i.e.  $\arg(\delta_{\text{LR}}) \sim 4.3-2\pi$ ,  $\arg(\delta_{\text{RL}}) \sim 1.2-3.2$ ,  $\text{Br}(\pi^+\pi^-)$  can be brought down by SUSY contributions to the experimental range. The strength factor of  $a_{\rho\gamma}$  [33, 36],

$$\sin 2\theta \equiv \frac{2|C_\gamma C'_\gamma|}{|C_\gamma|^2 + |C'_\gamma|^2}, \quad (27)$$

can be as large as 90% in this case. The measurability of the asymmetry in  $B \rightarrow \rho\gamma$  decay is better than in  $B \rightarrow K^*\gamma$ , since it readily provides vertex information [36].

It is clear from Fig. 6 that we might as well take  $m_{\tilde{g}} = 500$  GeV,  $\tilde{m} = 900$  and  $\delta_{\text{LR,RL}} = 0.006$ . The previous case corresponds to  $x_{\tilde{g}\tilde{q}} = 0.06$ , while in this case we have the larger value of  $x_{\tilde{g}\tilde{q}} = 0.31$ . These two cases also represent other cases with similar  $x_{\tilde{g}\tilde{q}}$ , while  $\tilde{m}$  need not be

that heavy. The figures for  $\text{Br}(\pi^+\pi^-)$  are almost identical to Fig. 7. However, as we show in Fig. 8a, the latter case has a greater  $\text{Br}(\rho^0\gamma)$ . Note that RL case is insensitive to  $\arg(\delta_{\text{RL}})$ , since the rate is proportional to  $|C_\gamma|^2 + |C'_\gamma|^2$ . In this case,  $\text{Br}(\rho^0\gamma) = \text{Br}^{\text{SM}}(\rho^0\gamma) + \text{Br}^{\text{SUSY}}(\rho^0\gamma)$  is within 5 times the SM rate as required by Figs. 5 and 6. The whole  $B \rightarrow \pi\pi$  favored range,  $\arg(\delta_{\text{RL}}) \sim 1.2-3.2$  is also allowed by the  $B \rightarrow \rho\gamma$  constraint. The  $\sin 2\theta$  is 80%. For the LR case, the induced  $C_\gamma^{\text{SUSY}}$  may have constructive or destructive interference with  $C_\gamma^{\text{SM}}$  as  $\arg(\delta_{\text{LR}})$  changes. Within the range of  $\arg(\delta_{\text{LR}}) \sim 4.3-2\pi$ , allowed by the  $B \rightarrow \pi\pi$  rate, there is quite some parameter space to satisfy the  $B \rightarrow \rho\gamma$  constraint. The rate can be close to the SM expectation. In Fig. 8b, we show the asymmetry,  $a_{\pi^+\pi^-}$ . Note that the SUSY prediction for  $a_{\pi^+\pi^-}$  from the previous two parameter points are close as in the  $\text{Br}(\pi^+\pi^-)$  case. In the generalized factorization,  $a_{\pi^+\pi^-}^{\text{SM}} \sim 3.3\%$  with our input parameter, a smaller  $\langle q^2 \rangle$  will have a slightly larger asymmetry. With SUSY,  $a_{\pi^+\pi^-}$  can be ranging within  $-1\%$  to  $8\%$ . Note that in the QCD factorization approach including a weak annihilation contribution  $a_{\pi^+\pi^-}^{\text{SM}} \sim -5\%$  to  $15\%$ , for  $\phi_3 \sim 60^\circ$  [16]. It is difficult to distinguish SUSY contributions from the SM prediction from  $a_{\pi^+\pi^-}$ .

## 4 Discussion

Left–left and/or right–right [8]  $\tilde{d}-\tilde{b}$  mixings with a few% to a few 10% mixing angle can generate a large enough contribution to  $B_d$  mixing to reduce  $a_{J/\psi K_S}$  from its SM value. As shown in Fig. 4b, such squark mixing angles are safe as regards the  $B \rightarrow \rho\gamma$  constraint. However, as shown in Fig. 4a, one needs large mixing with a sizable mass splitting to affect the  $B \rightarrow \pi\pi$  decay rate in this case. Such a large mixing is already ruled out by the experimental measurement of  $\Delta m_{B_d}$ , as shown in Figs. 1a and 1b, unless one fine tunes the parameter space to be very close to  $x_{\tilde{g}\tilde{q}} = 2.43$ , and turn off left–left or right–right mixings. In other words, one needs a high degree of fine tuning to account for both the low  $\sin 2\phi_1$  and  $B \rightarrow \pi\pi$  decay rate with LL or RR mixings. It is much easier to compete with the SM box diagram and modify  $\sin 2\phi_1$  than to compete with tree dominated  $B \rightarrow \pi\pi$  decay.

Alternatively, left–right and/or right–left  $\tilde{d}-\tilde{b}$  mixings with a few% mixing angles could also give a sizable contribution to  $B_d$  mixing. However, because of the amplification effect of the chiral enhancement, the size of this mixing angle is severely constrained by  $B \rightarrow \rho\gamma$  to be less than 2% in most of the parameter space given in Fig. 5b. It cannot be the source that gives a sizable contribution to  $B_d$  mixing, as one can tell by comparing Figs. 2 and 5b. It is interesting that, as noted already in the previous section, there is a parameter space where  $m_{\tilde{g}}$  is suitably light and the mixing angle  $\delta_{\text{LR,RL}}$  is less than 1%, where the model gives a sizable contribution to  $B \rightarrow \pi\pi$  decay without violating the  $B \rightarrow \rho\gamma$  constraint. In other words, we need left–right and/or right–left mixings rather than left–left and/or right–right mixings to affect  $B \rightarrow \pi\pi$  decay. Thus, if the smallness of  $\text{Br}(B \rightarrow \pi\pi)$  is due to SUSY,



it is likely that one will have large effects in  $b \rightarrow d\gamma$ , including rate enhancement and mixing induced asymmetry [36], which can easily be close to 100%.

In Sect. 3, we used  $\phi_3 = 65^\circ$ , which is a CKM fit-like value, since the SUSY contribution to  $B \rightarrow \pi\pi$  decay is uncorrelated with the SUSY contribution to  $B_d$  mixing. The CKM fit may still be viable and need not support a large  $\phi_3$  as a solution of the low  $B \rightarrow \pi\pi$  rate.

It is clear that we still need correct interference patterns, i.e. correct SUSY phases, to reduce  $a_{J/\psi K_S}$  and  $\text{Br}(B^0 \rightarrow \pi^+\pi^-)$ . Since these effects arise from different squark mixing sources, one can always find separate SUSY phases to achieve this. As we show in Sects. 2 and 3, we may have an accessible allowed region on SUSY phases.

## 5 Conclusions

We have shown that it is possible for SUSY models to account for the smaller  $\sin 2\phi_1$  and  $\text{Br}(B \rightarrow \pi\pi)$  values that seem to be emerging from the  $B$  factories. However, they would have to come from different flavor mixing sources. The smallness of  $\sin 2\phi_1$  is most likely arising from left–left (right–right) squark mixing, while the deficit in  $\text{Br}(B \rightarrow \pi\pi)$  is most likely due to left–right squark mixings. The two are basically uncorrelated.

Because of the similarity in chiral enhancement, the loop induced  $b \rightarrow d\gamma$  process is even more sensitive to  $\delta_{LR,RL}$  than the tree dominated  $B \rightarrow \pi\pi$  decay. Therefore, if SUSY affects the latter, the effects in the former would be even more prominent. We emphasize that  $B \rightarrow \rho\gamma$  could be considerably larger than expected in SM if the smallness of  $B \rightarrow \pi\pi$  rate is in part due to SUSY.

*Acknowledgements.* A.A. is on leave of absence from Department of Mathematics FSTT, P.O. Box 416, Tangier, Morocco. This work is supported in part by NSC-89-2112-M-002-063, NSC-89-2811-M-002-0086 and 0129, the MOE CosPA Project, and the BCP Topical Program of NCTS.

## References

1. T. Affolder et al. [CDF Collaboration], Phys. Rev. D **61**, 072005 (2000) [hep-ex/9909003]
2. K. Ackerstaff et al. [OPAL collaboration], Eur. Phys. J. C **5**, 379 (1998) [hep-ex/9801022]
3. R. Barate et al. [ALEPH Collaboration], Phys. Lett. B **492**, 259 (2000) [hep-ex/0009058]
4. A. Abashian et al. [BELLE Collaboration], Phys. Rev. Lett. **86**, 2509 (2001) [hep-ex/0102018]
5. B. Aubert et al. [BABAR Collaboration], Phys. Rev. Lett. **86**, 2515 (2001) [hep-ex/0102030]
6. M. Ciuchini et al., hep-ph/0012308
7. A. Ali, D. London, Eur. Phys. J. C **18**, 665 (2001) [hep-ph/0012155]
8. C.-K. Chua, W.-S. Hou, Phys. Rev. Lett. **86**, 2728 (2001) [hep-ph/0005015]
9. D. Cronin-Hennessy et al. [CLEO Collaboration], Phys. Rev. Lett. **85**, 515 (2000)
10. A. Hoecker, talk presented at BCP4 (Ise, Japan, February 2001)
11. T. Iijima, talk presented at BCP4 (Ise, Japan, February 2001)
12. D.G. Hitlin [BABAR Collaboration], plenary talk at ICHEP2000 (Osaka 2000), to appear in the Proceedings, hep-ex/0011024
13. P. Chang, talk presented at ICHEP2000 (Osaka 2000), to appear in the Proceedings
14. A. Ali, G. Kramer, C. Lu, Phys. Rev. D **58**, 094009 (1998) [hep-ph/9804363]
15. M. Beneke, G. Buchalla, M. Neubert, C.T. Sachrajda, Phys. Rev. Lett. **83**, 1914 (1999) [hep-ph/9905312]; T. Muta, A. Sugamoto, M. Yang, Y. Yang, Phys. Rev. D **62**, 094020 (2000) [hep-ph/0006022]
16. M. Beneke, G. Buchalla, M. Neubert, C.T. Sachrajda, hep-ph/0104110
17. See, for example, H.E. Haber, G.L. Kane, Phys. Rept. **117**, 75 (1985)
18. F. Gabbiani et al., Nucl. Phys. B **477**, 321 (1996)
19. S. Bertolini, F. Borzumati, A. Masiero, Nucl. Phys. B **294**, 321 (1987); S. Bertolini, F. Borzumati, A. Masiero, G. Ridolfi, Nucl. Phys. B **353**, 591 (1991)
20. G. 't Hooft, Nucl. Phys. B **72**, 461 (1974)
21. G.C. Branco, G.C. Cho, Y. Kizukuri, N. Oshimo, Phys. Lett. B **337**, 316 (1994) [hep-ph/9408229]; Nucl. Phys. B **449**, 483 (1995)
22. L.J. Hall, V.A. Kostelecky, S. Raby, Nucl. Phys. B **267**, 415 (1986)
23. J.A. Bagger, K.T. Matchev, R.-J. Zhang, Phys. Lett. B **412**, 77 (1997) [hep-ph/9707225]
24. A.J. Buras, in Probing the Standard Model of Particle Interactions, edited by F. David, R. Gupta (Elsevier Science B.V.), hep-ph/9806471
25. The LEP B Oscillation Working Group, <http://lepbose.web.cern.ch/LEPBOSC/>, results for the winter 2001 conferences (XXXVIth Rencontres de Moriond, Les Arcs, March 2001)
26. T. Draper, Nucl. Phys. Proc. Suppl. **73**, 43 (1999) [hep-lat/9810065]; S.R. Sharpe, hep-lat/9811006; Bernard, Nucl. Phys. Proc. Suppl. **94**, 159 (2001) [hep-lat/0011064]
27. N.G. Deshpande, X. He, J. Trampetic, Phys. Lett. B **377**, 161 (1996) [hep-ph/9509346]
28. X.-G. He, W.-S. Hou, K.-C. Yang, Phys. Rev. Lett. **81**, 5738 (1998) [hep-ph/9809282]
29. K.-C. Yang, talk presented at The International Workshop on  $B$  Physics and  $CP$  Violation (Taipei, June, 2001); private communication
30. A.L. Kagan, Phys. Rev. D **51**, 6196 (1995) [hep-ph/9409215]; M. Ciuchini, E. Gabrielli, G.F. Giudice, Phys. Lett. B **388**, 353 (1996) [Erratum *ibid.* B 393 (1996) 489] [hep-ph/9604438]
31. A.J. Buras, M. Misiak, M. Munz, S. Pokorski, Nucl. Phys. B **424**, 374 (1994) [hep-ph/9311345]
32. K. Fujikawa, A. Yamada, Phys. Rev. D **49**, 5890 (1994); P. Cho, M. Misiak, *ibid.* D **49**, 5894 (1994) [hep-ph/9310332]
33. C.-K. Chua, X.-G. He, W.-S. Hou, Phys. Rev. D **60**, 014003 (1999) [hep-ph/9808431]
34. Y. Ushiroda [Belle collaboration], talk presented at BCP4 (Ise, Japan, February 2001), hep-ex/0104045
35. M. Nakao, talk presented at ICHEP2000 (Osaka, 2000), to appear in proceedings
36. D. Atwood, M. Gronau, A. Soni, Phys. Rev. Lett. **79**, 185 (1997) [hep-ph/9704272]